



On the promotion of high temperature AP decomposition with silica mesoparticles

Haiyang Wang, Miles C. Rehwoldt, Xizheng Wang, Yong Yang, Michael R. Zachariah*

Department of Chemical and Biomolecular Engineering and Department of Chemistry and Biochemistry, University of Maryland, College Park, MD 20742, United States

ARTICLE INFO

Article history:

Received 18 July 2018

Revised 20 November 2018

Accepted 20 November 2018

Keywords:

Reactive materials

Silica

Catalysis

ABSTRACT

Silica particles are known to enhance the combustion of aluminum (Al) and ammonia perchlorate (AP) based energetic materials although the role of silica remains unknown. In this paper, AP/SiO₂ mesoparticles ((AP/SiO₂)_m) and Al/(AP/SiO₂)_m composite particles were prepared and the thermal properties/reactivity evaluated. Composites with 7 wt% SiO₂ have a reactivity ~7 times higher than that of Al/AP. The ignition temperature of Al/(AP/SiO₂)_m was also found to be ~100 °C lower compared to that of Al/AP. The thermal decomposition process of (AP/SiO₂)_m and Al/(AP/SiO₂)_m composite particles were investigated using both low and high heating rates. During slow heating, with the addition of silica, the decomposition of AP transitioned from a slow two-stage to a rapid one-step process. At high heating rate, the release temperature of ClO₂ and O₂ from AP is below ~400 °C, while for (AP/SiO₂)_m case, the peak release temperature is much higher at ~650 °C, when Al NPs reach its melting point and are ready to react. This may explain why Al/(AP/SiO₂)_m shows higher reactivity than Al/AP composite particles.

© 2018 Published by Elsevier Inc. on behalf of The Combustion Institute.

1. Introduction

Solid propellants with a wide range of burning rates [1] have been developed although only a few have found widespread application. One common formulation [1] consists of ammonium perchlorate (AP, oxidizer), aluminum (Al, fuel) and hydroxyl-terminated polybutadiene (HTPB, binder) as the primary components [2,3]. More recently, new binders such as glycidyl azide polymer (GAP) [4,5] and polyvinylidene fluoride (PVDF) [4] have attracted increasing attention because they not only act as binders but also participate in the energy release. Significant effort have been invested to tune the burning rate by increasing the thermal conductivity with embedded metal wires [6], graphene sheets [7–9], and replacing micro-sized components with nano-sized ones [10–13]. Catalysts such as iron oxide and copper oxide have also been added [4,5] to promote the decomposition of AP. Additionally, by achieving high interfacial area between catalyst and AP as well as raising the contact area between the Al and AP, the burning of the propellant can be promoted [2,14–22]

One of the key factors that affect the propagation velocity is the mode and facility of heat transfer. As mentioned above, enhancing heat conduction with the incorporation of metal wire or graphene has been shown to promote the burning rate [6–9].

However, oddly, there are reports that adding a low heat conductive material, thought to be chemically inert, has been observed to increase the burning of propellants of AP based energetic materials [17,23–25]. Romodanova and Pokhil [23] measured the burning rates of Al/AP with different additives and found that a 1 wt% addition of SiO₂ was the most efficient burning rate promoter at both low and high pressures, superior to both Fe₂O₃ and V₂O₅. The authors suggested that the silica disturbs the integrity of the Al oxide shell, promoting the oxygen access to the metal fuel [23]. Shioya et al. [24] added a silica-based, diatomaceous earth (88 wt% SiO₂) into a propellant and found ignitability and burning characteristics were both enhanced. They proposed that the low thermal conductivity of SiO₂ promoted the formation of hot spots [24]. Both the above two studies suggest a physical enhancement mechanism of SiO₂ on the combustion of Al/AP. However, Luo and coworkers [17] found that the addition of SiO₂ cryogel boosts the decomposition of AP and increases its heat release. In our previous work, the burning rate of Al/PVDF film with 5 wt% mesoporous silica was found to be three times higher compared to that of Al/PVDF without silica [25]. Further investigation shows that mesoporous silica promoted the decomposition of PVDF, suggesting a synergetic chemical and physical effects. It is noted that the objective of these studies is not to create a propellant with high energy density since silica is an inert component which reduces the total energy density [17,23–25].

In this paper, to investigate the role of silica in Al/AP based energetic materials, a close-assembly of (AP/SiO₂)_m was prepared by

* Corresponding author.

E-mail address: mrz@umd.edu (M.R. Zachariah).

a spray-drying process and then mixed with Al NPs to form an Al/(AP/SiO₂)_m composite. The effect of silica on the thermal decomposition of AP and Al/AP was investigated by slow and high heating rate techniques. And the reactivity of Al/(AP/SiO₂)_m composite was also evaluated in a confined combustion cell. The composites with 7 wt% SiO₂ showed a ~7 times higher reactivity and a lower ignition temperature (100 °C lower) than conventional Al/AP. Further investigation found that silica nanoparticles promote the decomposition of AP with enhanced O₂ and ClO₂ generation at the point where Al NP's melt.

2. Experimental section

2.1. Chemicals

Al NPs (~85 nm, 81 wt% active aluminum, confirmed by TG) were purchased from Novacentrix. Ammonium perchlorate (AP, ~170 μm, 99.8 wt%) was purchased from Sigma-Aldrich Corp. Colloidal silica (SNOWTEX ST-PS-S, 15–16 wt% SiO₂) was purchased from Nissan Chemical Industries, and Ltd. Hexane (BDH, 98.5% n-hexane) was purchased from VWR International. All chemicals were used as received.

2.2. Preparation of fine AP and AP/SiO₂ mesoparticles ((AP/SiO₂)_m)

AP fine particles (~1 μm, Fig. S1) were prepared by conventional spray drying [26]. An AP aqueous solution with 5 wt% AP (commercial AP dissolves in deionized water) was aerosolized by an atomizer with dry air (~35 psi) and passed through a silica gel tube to dehydrate, followed by a complete dehydration in a tube furnace at 150 °C. The obtained fine AP powders were collected on a membrane filter with a pore size of ~0.4 μm and stored at ~85 °C to prevent morphological changes due to its hygroscopicity. The silica gel was baked at ~80 °C overnight before using. For (AP/SiO₂)_m preparation (Fig. 1a), commercial AP particles and colloidal silica were dissolved and dispersed in deionized water (DI water), respectively. After 30 min sonication and 24 hour stirring, the colloidal solution was spray dried at 150 °C to obtain (AP/SiO₂)_m. The prepared AP and (AP/SiO₂)_m particles are shown in Figs. S1 and S2.

2.3. Preparation of physically mixed Al/AP and Al/(AP/SiO₂)_m composites

The Al/AP and Al/(AP/SiO₂)_m composite particles were prepared by a conventional physical mixing method. A stoichiometric ratio of Al and AP (or (AP/SiO₂)_m) was weighed and added to a vial with 10 mL hexane. Note that silica is counted as an additive rather than an oxidizer when calculating the ratio. After 30 min ultrasonication, the uncovered vial was placed in a fume hood overnight to dry. Then the dry powders were broken gently with a spatula. All the thermite samples were stored in a desiccator.

2.4. Structure characterization

The mesoparticles and composite particles were characterized using a Hitachi SU-70 scanning electron microscope (SEM) coupled to an energy dispersive spectrometer (EDS). The (AP/SiO₂)_m were also characterized by transmission electron microscopy (TEM) (JEOL 2100F field-emission instrument). The crystal structures of the (AP/SiO₂)_m with different SiO₂ content were characterized by powder X-ray diffraction (XRD, Bruker D8 with Cu K radiation). Le Bail refinements of all the patterns were performed with the TOPAS 4.2 software [27] to obtain their crystallite size and cell volume.

2.5. Thermal decomposition properties

Thermogravimetry/differential scanning calorimetry (TGA/DSC) results were obtained with a TA Instruments Q600 in an argon atmosphere (flow rate: 100 mL/min) coupled to a mass spectrometer (MS) with a heating rate of 5 °C/min. The mass loading was ~5 mg, and the heat flow was normalized by mass. Heating rates (1, 2, 4, and 8 °C/min) were varied for both AP and AP/SiO₂ samples (in argon with a flow rate of 100 mL/min) to calculate the apparent activation energy of decomposition with the different reaction content by Ozawa method [28–30]. Derivative thermogravimetric analysis (DTG) result was obtained by taking the derivative of TGA curve.

Temperature-Jump/Time-of-Flight mass spectrometry (T-Jump/TOFMS) was used to characterize the species released during fast heating. The details of T-Jump/TOFMS system can be found in the reference [31]. Typically, a ~10 mm long platinum (Pt) filament (~76 μm in diameter) coated with the sample (~4 mm long) was resistively heated to ~1200 °C (heating rate of ~1.2 × 10⁵ °C s⁻¹).

2.6. Combustion cell measurements

The details of the combustion cell experiment can be found in our previous study [32]. The combustion cell has a constant volume of ~20 cm³, in which a pressure sensor and an optical emission sensor were built in. For a typical experiment, 25.0 mg of sample was placed in the cell and ignited by joule heating with a nichrome coil. Once ignited, the pressure-time and optical emission-time curves were recorded by the sensors and processed by the data acquisition devices. The pressurization rate (dP/dt) is defined as the initial slope of the pressure rise, and the FWHM burn time is defined as the full-width half-maximum of the optical emission curve. For one sample, the experiments were replicated in triplicate. Peak pressure represents to the gas generating ability of measured energetic materials, while pressure rise rate corresponds to the burn rate and burn time has inverse correlation to burn rate.

3. Results and discussions

3.1. Preparation of AP and (AP/SiO₂)_m

(AP/SiO₂)_m particles with different silica content were prepared by a spray-drying process, as shown in Fig. 1a. The SEM, EDS, and TEM images of the formed (AP/SiO₂)_m with 20 and 50 wt % silica are shown in Fig. 1 (AP/SiO₂ at other ratios are shown in Fig. S2). As the SEM images (Fig. 1b and c) show, the prepared particles are spherical with a size distribution of 0.2–2 μm (average ~1 μm). Individual AP crystals were not observed to form (SEM, and the EDS results in Fig. 1b-1 and 1c-1) indicating that the AP was distributed homogeneously within the whole mesoparticle. TEM images reveal that nano-silica particles (~10–15 nm) form mesoparticles with the AP embedded into the mesoporous structure. The (AP/SiO₂)_m with 20 wt% silica showed larger pores compared to 50 wt% because of larger loading of AP. Compared to the AP fine particle which has an issue of storage because of its hygroscopicity [33], the prepared (AP/SiO₂)_m are stable without any morphology change in the atmosphere for 2 months (Figs. S1 and S2).

The XRD patterns for commercial AP, sprayed fine AP (without silica, the same process as above), and (AP/SiO₂)_m with different of SiO₂ content (10–70 wt%) are shown in Fig. 2a. As the figure shows, only single-phase AP (PDF#: 43-0648) was detected in the XRD, as the silica is amorphous. Nevertheless, the AP XRD is sensitive to the mass fraction of silica employed. Increasing silica content means closer packing of nanoparticles which provides higher surface area for the nucleation of AP crystallization but leaves smaller

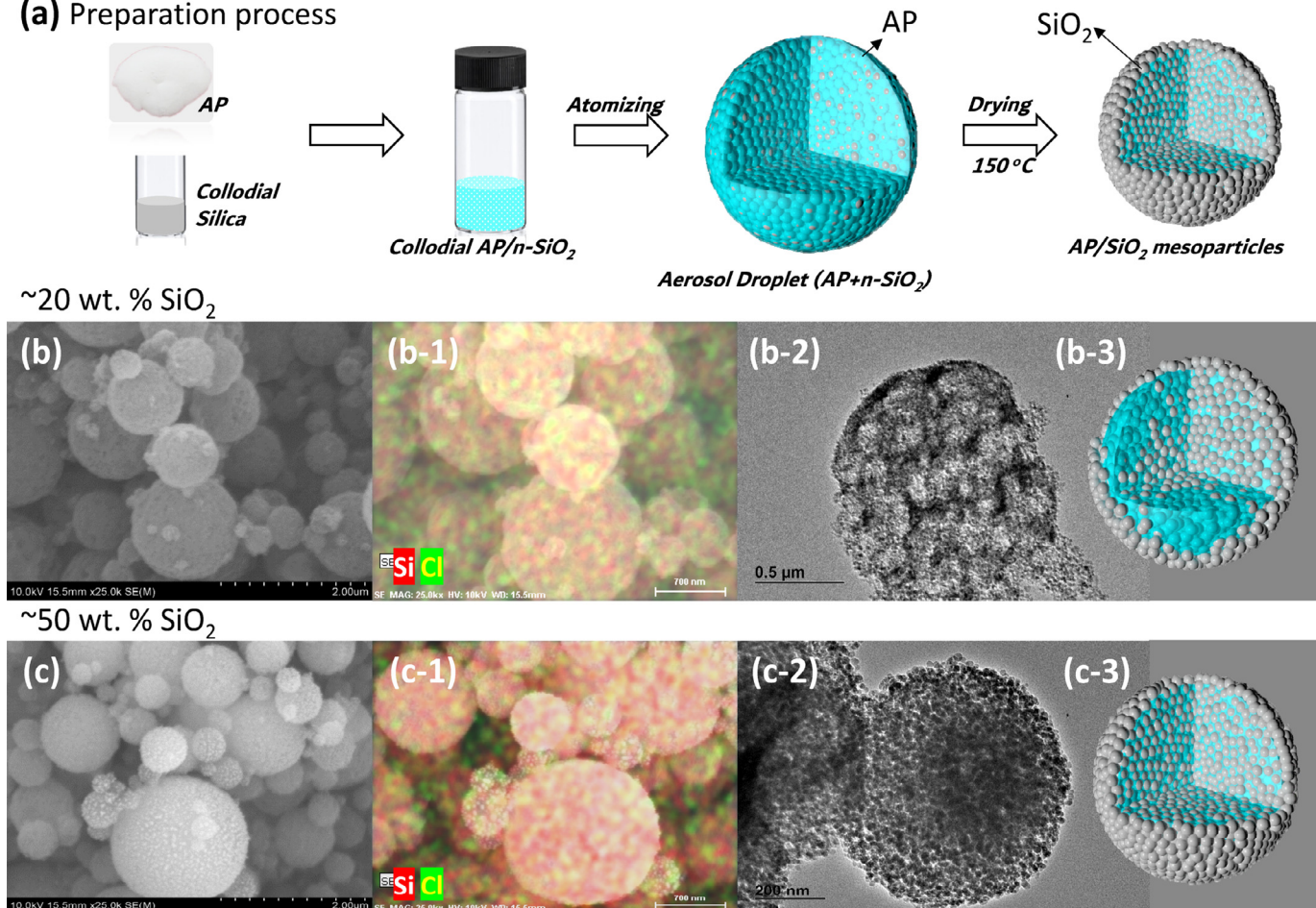
(a) Preparation process

Fig. 1. Preparation approach (a), SEM (b, c), EDS mapping (b-1, c-1), TEM (b-2, c-2) and schematic showing (b-3, c-3) (AP/SiO₂)_m with different silica content (b, 20 wt% silica; c, 50 wt% silica).

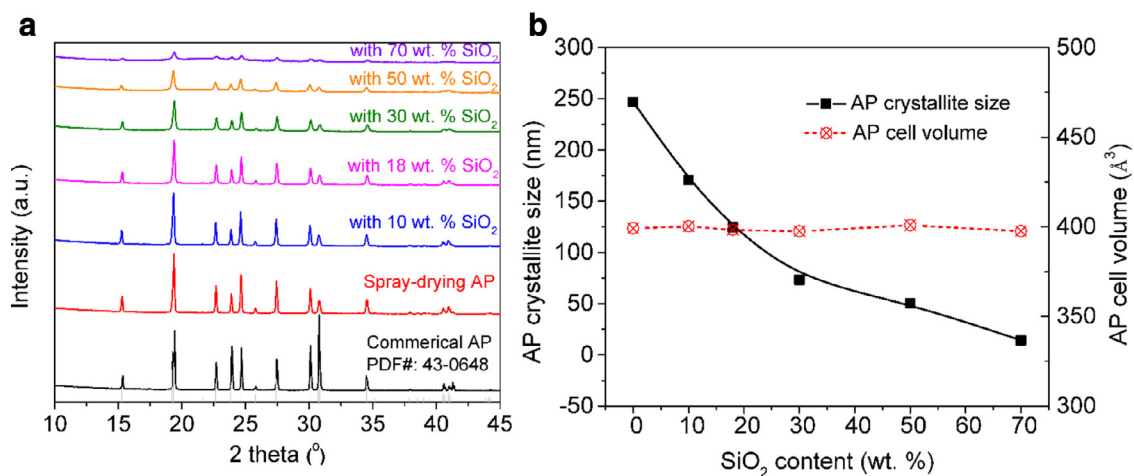


Fig. 2. XRD (a) commercial AP, spray-dried AP and (AP/SiO₂)_m with various silica content. (b) Calculated AP crystallite size and AP cell volume of AP/SiO₂ with various silica content. (Note: Silica content changes from 0 wt% to 70 wt%).

spaces for growth, as evidenced by the broader peaks. Le Bail refinements by the TOPAS 4.2 software gives the crystalline size and cell volume as a function of silica loading and are plotted in Fig. 2b. With the increase of silica content, the crystallite size of AP decreases from ~250 nm to ~20 nm while the cell volume remains constant at ~400 Å³. Thus, the mesoporous silica, within which the AP is integrated, serves as a matrix to limit the growth of AP crystals, resulting in reduced crystalline size.

3.2. Reactivity of Al/(AP/SiO₂)_m composite particles

The fine AP particles and (AP/SiO₂)_m were physically mixed with Al NPs and the dry powders (Fig. S3) were ignited in the combustion cell. The peak pressure/pressure rise rate and the burning time results are shown in Fig. 3a and b, respectively. From Fig. 3a, we can see that both the peak pressure and pressure rise rate increase linearly from 2 to 7 wt% silica. The peak

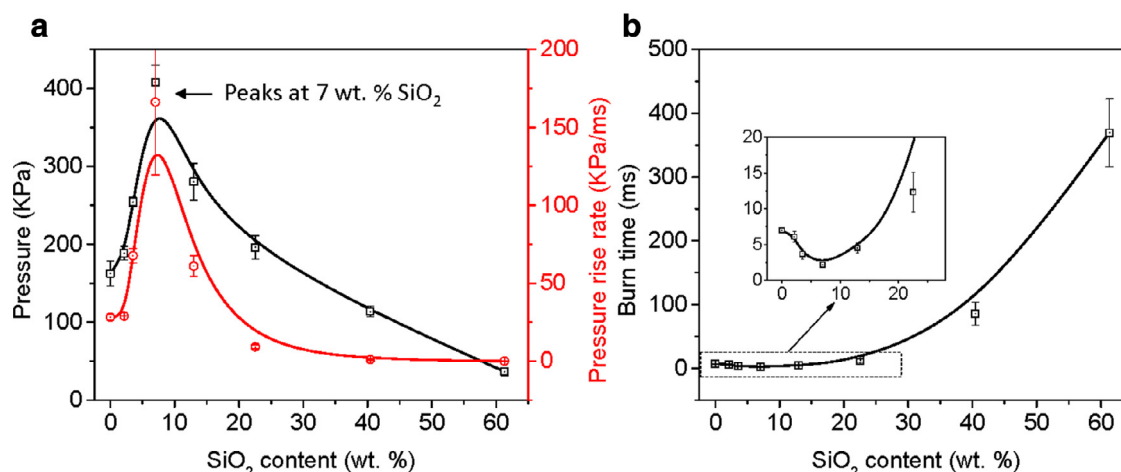


Fig. 3. Peak pressure (a, square marker), pressure rise rate (a, round marker) and burn rate (b) of Al/(AP/SiO₂)_m composites with various contents of silica (0 wt% to ~60 wt%).

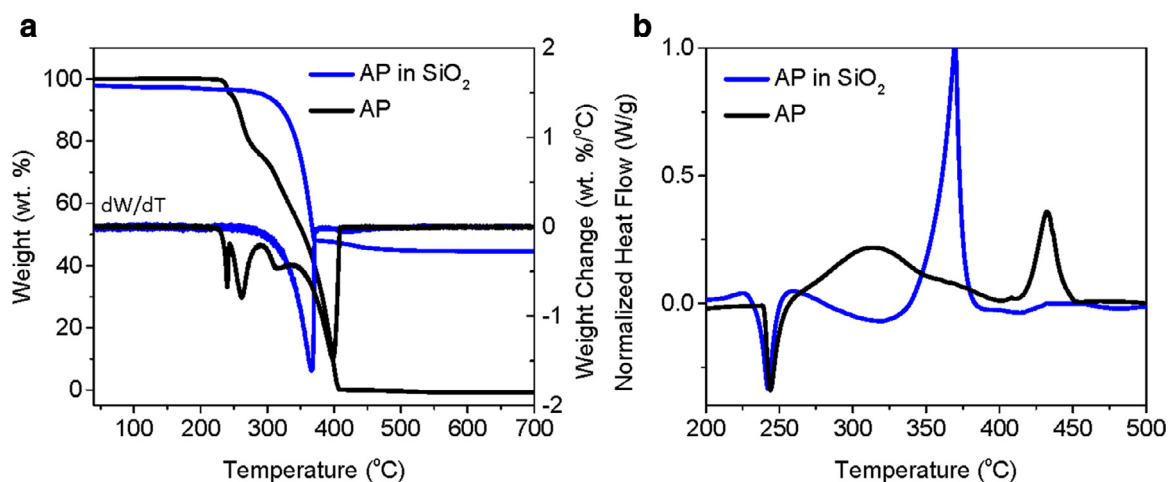


Fig. 4. TGA/DTG (a) and DSC (b) results of AP and (AP/SiO₂)_m (50 wt% silica) with a heating rate of 5 °C/min.

pressure and pressure rise rate of the 7 wt% case is $\sim 2.5\times$ and $\sim 7\times$ that of Al/AP without silica. Correspondingly, the burn time of the Al/(AP/SiO₂)_m composite (7 wt% silica) is only ~ 2 ms, which is $\sim 1/4$ of the Al/AP without silica case. As Fig. 3a shows, when the silica loading was increased further, both the peak pressure and pressure rise rate decreased rapidly. However, as Fig. 3a shows, the reactivity of the composites with 13 wt% silica is still higher than Al/AP.

3.3. Thermal decomposition of AP/SiO₂ (slow heating rate)

The thermal decomposition of (AP/SiO₂)_m (50 wt%) and neat fine AP, at low heating rates (TGA/DSC/MS, 5 °C/min) is shown in Fig. 4a and b. The decomposition of neat AP shows the familiar two stage decomposition (low and high temperature decomposition stages, LTD and HTD for short) [34–36] (~ 310 °C and 435 °C), however addition of silica (AP/SiO₂)_m occurs in a single step, with a peak at 370 °C. A well-accepted theory is that the decomposition of AP is triggered by proton transfer on the crystal surface, [34–36] followed by decomposition to NH₃ and HClO₄. While some NH₃ appears to be oxidized by the HClO₄ on the surface (where LTD comes from) but most of the surface generated NH₃ is absorbed into pores and accumulate around the crystals. The absorbed ammonia limits further proton transfer and thus passivates the surface of AP, retarding decomposition. As the temperature increases, NH₃ will be desorbed leading to the HTD decomposition [34–36]. It is also known smaller AP particles undergo a smaller

LTD and a larger HTD step [34–37]. Consequently, because the AP is embedded within the SiO₂ matrix mesoparticles and is thus much smaller (< 100 nm, Fig. 1b-2 and 1c-2), no obvious LTD is seen in Fig. 4a.

Another possible reason is that the AP crystals (< 100 nm) are locked in the mesoporous silica, since silica is a good adsorbent for ammonia [38–40], and thus, we observe very limited mass loss in the LTD region since the ammonia is fixed. When the temperature exceeds > 300 °C, ammonia is evolved, and this internal pressurization results in disassembling of the (AP/SiO₂)_m and rapid reaction between NH₃ and HClO₄, resulting in one-step decomposition of AP. The activation energy of AP and AP/SiO₂ obtained by the Ozawa method at heating rates of 1, 2, 4 and 8 °C/min are shown in Figs. S4 and S5, respectively. We find that AP/SiO₂ actually has a higher apparent activation energy (~ 130 kJ/mol) than neat AP (~ 100 kJ/mol), which initially sounds contrary to the general logical being presented, however, this higher activation energy is likely a manifestation of the elimination of the LTD stage and in any case the relative differences in activation are not sufficient to infer any major significance.

Evolved species including N₂O, O₂, NO₂ (or NO), H₂O and NH₃ from the decomposition of AP and (AP/SiO₂)_m are shown in Fig. 5a as a function of temperature under slow heating (5 °C/min in argon). Consistent with TGA, the LTD and HTD, are clearly observed for the neat AP, while in the presence of silica the LTD is lost and a narrower and more intense gas evolution peak is seen at

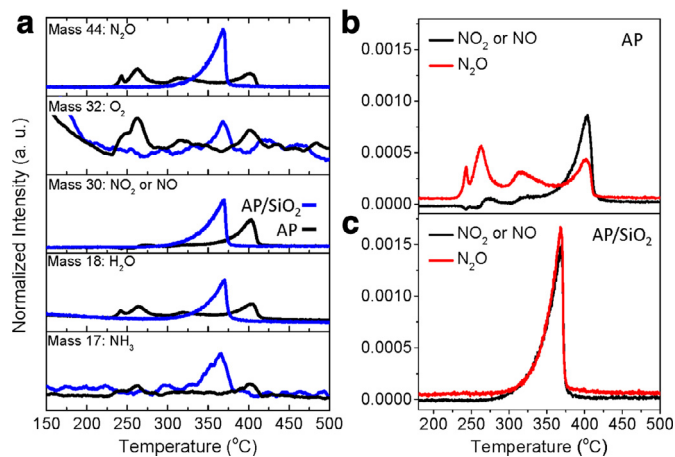


Fig. 5. MS results. Blue: AP/SiO₂; Black: AP (a), normalized (by mass of AP) NO₂ (or NO) and N₂O gas released from AP (b) AP/SiO₂)_m (c) at a heating rate of 5 °C/min. Note: The signal of NO₂ or NO (30) presented is after removal of the contribution from N₂O (44) fragmentation. The signal of NH₃ (17) presented is after removal of the contribution from H₂O (18) fragmentation to OH. The standard MS spectrum of N₂O (44) and H₂O (18) was obtained from the NIST-webbook. (For interpretation of the references to color in this figure legend, the reader is referred to the web version of this article.)

higher temperatures. As Fig. 5b shows, NO₂ is the primary reaction product initiating at ~370 °C consistent with prior results [34–36]. However, for AP/SiO₂ (Fig. 5c), NO₂ and N₂O were released simultaneously with similar intensity, clearly confirming a one-step decomposition.

3.4. Ignition of Al/AP and Al/(AP/SiO₂)_m composite particles (T-Jump fast heating rate)

The ignition of Al/AP and Al/(AP/SiO₂)_m composites (SEM images in Fig. S3) were investigated on a fast heating wire (Pt filament, ~76 μm in diameter), which was coated with the sample (~4 mm long) and resistively heated to ~1200 °C (heating rate of ~1.2 × 10⁵ °C s⁻¹) in argon, from which, ignition snapshots were recorded (76,000 frames per second) and the ignition temperature obtained, as shown in Fig. 6. Compared to Al/AP, the Al/(AP/SiO₂)_m (7 wt% silica) composites clearly show a much more violent reaction with a larger and brighter flame. The ignition temperatures of Al/AP and Al/(AP/SiO₂)_m (7 wt% silica) based on the ignition delay times are ~800 °C and ~700 °C, respectively. As the TG/DSC/MS results (Figs. 4 and 5) show, AP releases oxidants; N₂O and O₂, at a low temperature (~270 °C), but is actually too low for Al to react. The high melting point of Al (660 °C) leads to the long ignition delay till the HTD of AP, when NO₂ is released. As our previous study

shows [14], the Al/AP/NC composites (Al NPs were encapsulated in AP/NC matrix) ignited ~230 °C lower than the Al melting point. We found that Al/AP/NC released much more HCl, than Al/AP mixture, and this serves to etch alumina and lower the ignition temperature, by exposing the still solid Al fuel. In this study, while the ignition temperature was lowered it was still above the Al melting point, probably owing to the much larger distance between Al and AP in the physical mixture compared to the Al–AP core-shell structure.

3.5. T-Jump MS of Al/AP and Al/(AP/SiO₂)_m composite particles

The reaction dynamics under high heating rate were characterized by a T-jump/TOFMS with the temporal evolution of the highest concentration reaction products ClO₂, O₂, NH₃, HCl, HClO, NO₂ (or NO) and N₂O shown in Fig. 7. It is quite clear that Al/(AP/SiO₂)_m releases more ClO₂, O₂, HCl, and NH₃, compared to Al/AP case. It is noted here that the release of oxide gas species such as ClO₂, O₂, and NO₂ from Al/(AP/SiO₂)_m peak at ~600–700 °C, which overlaps the melting point of Al NPs (660 °C) when Al is ready to react. However, for the Al/AP particles, the oxide gas species were released maximally at ~400 °C, which is ~250 °C lower than Al melting point. Figure 7 also shows a much higher concentration of HCl from Al/(AP/SiO₂)_m composite particles, which is known to etch Al₂O₃ and promote ignition as discussed above [14]. Figure S6 confirms this interaction through SEM/EDS which shows chlorine in the combustion residue of Al/(AP/SiO₂)_m. The particle sizes of combustion residue of Al/(AP/SiO₂)_m (< 1 μm) were found to be smaller than those of Al/AP (> 5 μm), indicating less sintering of Al NPs occurred during combustion in Al/(AP/SiO₂)_m. This post analysis also indicates that the silica mesoparticle is not seen, indicating disintegration to the individual silica nanoparticles, ~10–15 nm, and are shown in Fig. S7.

3.6. Mechanism of Al/(AP/SiO₂)_m composite particles

We summarize our understanding of the mechanism of the ignition and combustion of Al/(AP/SiO₂)_m composite particles in Fig. 8. In a traditional Al/AP composition (Fig. 8a), the early stage LTD of AP has little impact since it occurs at a temperature too low for reaction with Al. It is only at the HTD step that ignition of Al is observed. For the Al/(AP/SiO₂)_m composite case however, shown in Fig. 8b, no obvious LTD step was observed, and ammonia is absorbed to silica. At or near the HTD a more violent gas release aided by absorbed ammonia results in disassembly of the silica mesoparticles preventing sintering and enhancing Al combustion. The enhanced HCl release should assist in weakening the Al₂O₃ shell and thus lowering the ignition temperature of Al NP's.

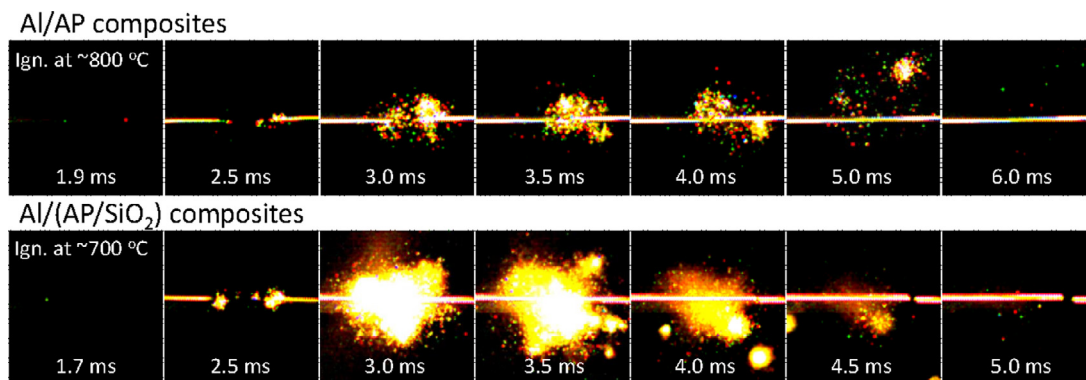


Fig. 6. T-Jump ignition of Al/AP and Al/(AP/SiO₂)_m (7 wt% silica) composites.

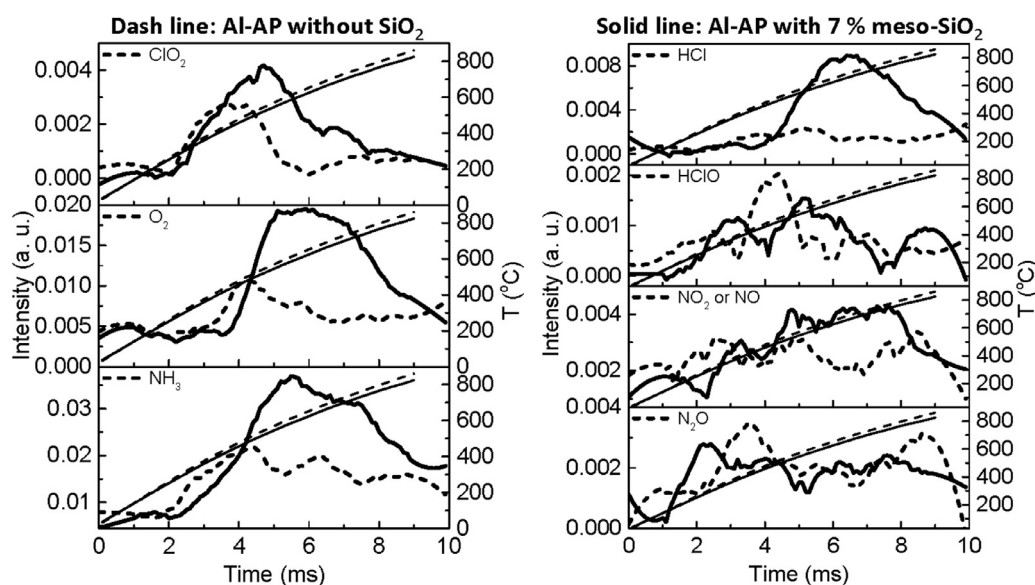


Fig. 7. T-Jump MS results of Al/AP (dash line) and Al/(AP/SiO₂)_m (7wt% silica, solid line) at a heating rate of 1.2×10^5 °C/s. Normalized to N₂ (28).

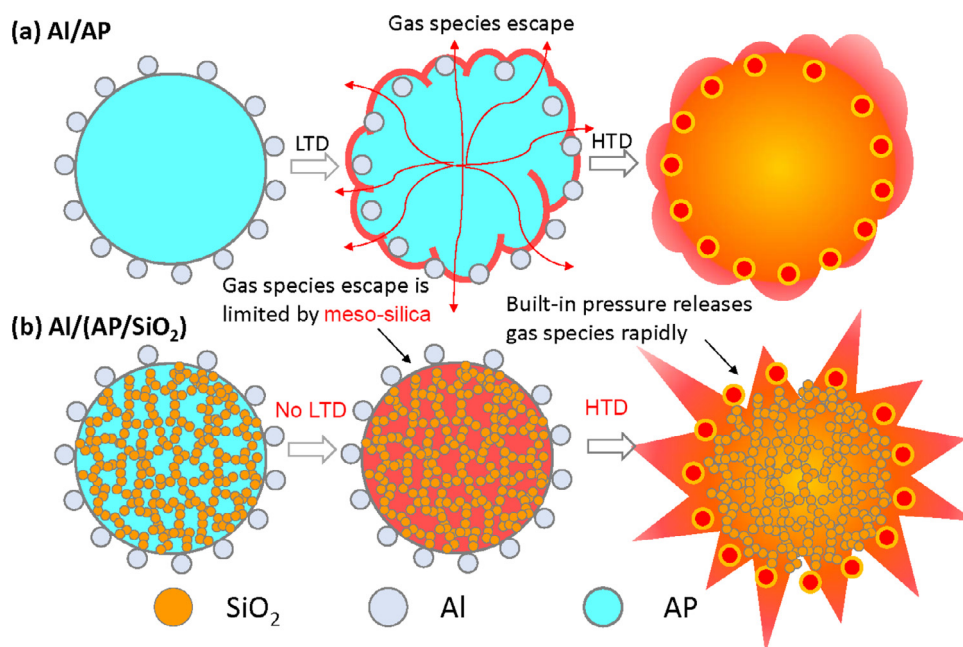


Fig. 8. Possible reaction mechanism of Al/AP and Al/(AP/SiO₂)_m (7wt% silica).

Even though SiO₂ has this benefit, it is worth to note that it is still an inert component which not only reduces the energy density of propellants when added but also reduce the reactivity when its content is > 15 wt% owing to heat-sink effect.

4. Conclusion

In this paper, (AP/SiO₂)_m with different SiO₂ content were prepared. We found that the Al/(AP/SiO₂)_m with 7 wt% SiO₂ has a reactivity of ~ 7 times higher than that of Al/AP while the peak pressure was > 2.5 times higher. The ignition temperature of Al/(AP/SiO₂)_m (7wt% SiO₂) was found to be ~ 100 °C lower compared to that of Al/AP, with a much more violent reaction. The decomposition process of AP and AP/SiO₂ composites were investigated by TGA/DSC/MS and T-Jump MS at both low and high heating rate, respectively. At low heating rate, (AP/SiO₂)_m decompose in one-step, with much higher NO₂ gas was released,

indicating a complete one-step high-temperature decomposition (HTD) compared to the typical two stages decomposition (LTD and HTD) in AP. At high heating rate, compared to Al/AP, Al/(AP/SiO₂)_m released much more ClO₂, O₂, and HCl, peaking at the temperature of ~ 600 – 700 °C, corresponding to the melting point of Al NPs (when Al is ready to react). Additionally, HCl gas released assists in etching the Al₂O₃ shell.

Acknowledgments

This work was supported by the Air Force office of Scientific Research.

We acknowledge the support of the Maryland Nanocenter and its NispLab. The NispLab is supported in part by the NSF as an MR-SEC Shared Experimental Facility.

Supplementary material

Supplementary material associated with this article can be found, in the online version, at doi:10.1016/j.combustflame.2018.11.021.

References

- [1] J.D. Hunley, The history of solid-propellant rocketry: What we do and do not know, 35th AIAA, ASME, SAE, ASEE Joint Propulsion Conference and Exhibit, Los Angeles, CA (1999), pp. 20–23.
- [2] K. Gnanaprakash, S.R. Chakravarthy, R. Sarathi, Combustion mechanism of composite solid propellant sandwiches containing nano-aluminium, *Combust. Flame* 182 (2017) 64–75.
- [3] Y. Chen, D.R. Guildenbecher, K.N.G. Hoffmeister, M.A. Cooper, H.L. Stauffacher, M.S. Oliver, E.B. Washburn, Study of aluminum particle combustion in solid propellant plumes using digital in-line holography and imaging pyrometry, *Combust. Flame* 182 (2017) 225–237.
- [4] C. Huang, G. Jian, J.B. DeLisio, H. Wang, M.R. Zachariah, Electro spray deposition of energetic polymer nanocomposites with high mass particle loadings: a prelude to 3D printing of rocket motors, *Adv. Eng. Mater.* 1 (2015) 95–101.
- [5] D.M. Badgular, M.B. Talawar, V.E. Zarko, P.P. Mahulikar, New directions in the area of modern energetic polymers: an overview, *Combust. Explos. Shock Waves* 4 (2017) 371–387.
- [6] N. Kubota, M. Ichida, T. Fujisawa, Combustion processes of propellants with embedded metal wires, *AIAA J.* 1 (1982) 116–121.
- [7] J.O. Hightower Jr, T. Sato, Solid rocket motor propellants with reticulated structures embedded therein to provide variable burn rate characteristics, U.S. Patent No. 4,756,251. 1988.
- [8] J.L. Sabourin, D.M. Dabbs, R.A. Yetter, F.L. Dryer, I.A. Aksay, Functionalized graphene sheet colloids for enhanced fuel/propellant combustion, *ACS Nano* 12 (2009) 3945–3954.
- [9] S. Isert, L. Xin, J. Xie, S.F. Son, The effect of decorated graphene addition on the burning rate of ammonium perchlorate composite propellants, *Combust. Flame* 183 (2017) 322–329.
- [10] Y. Kwon, A.A. Gromov, A.P. Ilyin, E.M. Popenko, G. Rim, The mechanism of combustion of superfine aluminum powders, *Combust. Flame* 4 (2003) 385–391.
- [11] L.T. De Luca, L. Galfetti, F. Severini, L. Meda, G. Marra, A.B. Vorozhtsov, V.S. Sedoi, V.A. Babuk, Burning of nano-aluminized composite rocket propellants, *Combust. Explos. Shock Waves* 6 (2005) 680–692.
- [12] R.W. Armstrong, B. Baschung, D.W. Booth, M. Samirant, Enhanced propellant combustion with nanoparticles, *Nano Lett.* 2 (2003) 253–255.
- [13] K. Jayaraman, K.V. Anand, S.R. Chakravarthy, R. Sarathi, Effect of nano-aluminum in plateau-burning and catalyzed composite solid propellant combustion, *Combust. Flame* 8 (2009) 1662–1673.
- [14] H. Wang, R.J. Jacob, J.B. DeLisio, M.R. Zachariah, Assembly and encapsulation of aluminum NP's within AP/NC matrix and their reactive properties, *Combust. Flame* 180 (2017) 175–183.
- [15] W. Zhao, T. Zhang, N. Song, L. Zhang, Z. Chen, L. Yang, Z. Zhou, Assembly of composites into a core-shell structure using ultrasonic spray drying and catalytic application in the thermal decomposition of ammonium perchlorate, *RSC Adv.* 75 (2016) 71223–71231.
- [16] G. Marothiya, C. Vijay, K. Ishitha, P.A. Ramakrishna, an effective method to embed catalyst on AP and its effect on the burn rates of aluminized composite solid propellants, *Combust. Flame* 182 (2017) 114–121.
- [17] R. Chen, Y. Luo, J. Sun, G. Li, Preparation and properties of an AP/RDX/SiO₂ nanocomposite energetic material by the sol-gel method, *Propellants Explos. Pyrotech.* 4 (2012) 422–426.
- [18] H. Shim, J. Kim, H. Kim, K. Koo, Production of the spherical nano-Al/AP composites by drowning-out/agglomeration and their solid-reaction kinetics, *Ind. Eng. Chem. Res.* 39 (2016) 10227–10234.
- [19] J. Dai, F. Wang, C. Ru, J. Xu, C. Wang, W. Zhang, Y. Ye, R. Shen, Ammonium perchlorate as an effective addition for enhancing the combustion and propulsion performance of Al/CuO nanothermites, *J. Phys. Chem. C* 18 (2018) 10240–10244.
- [20] Z. Ma, R. Wu, J. Song, C. Li, R. Chen, L. Zhang, Preparation and characterization of Fe₂O₃/ammonium perchlorate (AP) nanocomposites through ceramic membrane anti-solvent crystallization, *Propellants Explos. Pyrotech.* 2 (2012) 183–190.
- [21] D.A. Reese, S.F. Son, L.J. Groven, Preparation and characterization of energetic crystals with nanoparticle inclusions, *Propellants Explos. Pyrotech.* 6 (2012) 635–638.
- [22] Z. Ge, X. Li, W. Zhang, Q. Sun, C. Chai, Y. Luo, Preparation and characterization of ultrafine Fe-O compound/ammonium perchlorate nanocomposites via in-suit growth method, *J. Solid State Chem.* 258 (2018) 138–145.
- [23] L.D. Romodanova, P.K. Pokhil, Action of silica on the burning rates of ammonium perchlorate compositions, *Combust. Explos. Shock Waves* 3 (1970) 258–261.
- [24] S. Shioya, M. Kohga, T. Naya, Burning characteristics of ammonium perchlorate-based composite propellant supplemented with diatomaceous earth, *Combust. Flame* 2 (2014) 620–630.
- [25] H. Wang, J.B. DeLisio, S. Holdren, T. Wu, Y. Yang, J. Hu, M.R. Zachariah, Mesoporous silica spheres incorporated aluminum/poly (vinylidene fluoride) for enhanced burning propellants, *Adv. Eng. Mater.* 2 (2018) 1700547.
- [26] Y. Liang, H. Tian, J. Repac, S. Liou, J. Chen, W. Han, C. Wang, S. Ehrman, Colloidal spray pyrolysis: a new fabrication technology for nanostructured energy storage materials, *Energy Storage Mater.* 13 (2018) 8–18.
- [27] R.W. Cheary, A. Coelho, A fundamental parameters approach to X-ray line-profile fitting, *J. Appl. Crystallogr.* 2 (1992) 109–121.
- [28] S. Vyazovkin, A.K. Burnham, J.M. Criado, L.A. Pérez-Maqueda, C. Popescu, N. Sbirrazzuoli, ICTAC kinetics committee recommendations for performing kinetic computations on thermal analysis data, *Thermochim. Acta* 1–2 (2011) 1–19.
- [29] W. Zhou, J.B. DeLisio, X. Wang, G.C. Egan, M.R. Zachariah, evaluating free vs bound oxygen on ignition of nano-aluminum based energetics leads to a critical reaction rate criterion, *J. Appl. Phys.* 11 (2015) 114303.
- [30] G. Jian, L. Zhou, N.W. Piekielek, M.R. Zachariah, Low effective activation energies for oxygen release from metal oxides: evidence for mass-transfer limits at high heating rates, *ChemPhysChem* 8 (2014) 1666–1672.
- [31] L. Zhou, N. Piekielek, S. Chowdhury, M.R. Zachariah, T-Jump/time-of-flight mass spectrometry for time-resolved analysis of energetic materials, *Rapid Commun. Mass Spectrom.* 1 (2009) 194–202.
- [32] K. Sullivan, M. Zachariah, Simultaneous pressure and optical measurements of nanoaluminum thermites: investigating the reaction mechanism, *J. Propuls. Power* 3 (2010) 467–472.
- [33] C. Wu, K. Sullivan, S. Chowdhury, G. Jian, L. Zhou, M.R. Zachariah, Encapsulation of perchlorate salts within metal oxides for application as nanoenergetic oxidizers, *Adv. Funct. Mater.* 1 (2012) 78–85.
- [34] L. Mallick, S. Kumar, A. Chowdhury, Thermal decomposition of ammonium perchlorate-A TGA-FTIR-MS study. Part I, *Thermochim. Acta* 610 (2015) 57–68.
- [35] L. Mallick, S. Kumar, A. Chowdhury, Thermal decomposition of ammonium perchlorate-A TGA-FTIR-MS study. Part II, *Thermochim. Acta* 653 (2017) 83–96.
- [36] Y. Zhu, H. Huang, H. Ren, Q. Jiao, Kinetics of thermal decomposition of ammonium perchlorate by TG/DSC-MS-FTIR, *J. Energy Mater.* 1 (2013) 16–26.
- [37] R. Behrens, L. Minier, The thermal decomposition behavior of ammonium perchlorate and of an ammonium-perchlorate-based composite propellant, Sandia National Labs, Livermore, CA, United States, 1998 No. SAND-97-8422C; CONF-961194.
- [38] P. Ávan Der Voort, Reaction of NH₃ with trichlorosilylated silica gel: a study of the reaction mechanism as a function of temperature, *J. Chem. Soc. Faraday Trans.* 14 (1993) 2509–2513.
- [39] R. Roque-Malherbe, F. Marquez-Linares, W. Del Valle, M. Thommes, Ammonia adsorption on nanostructured silica materials for hydrogen storage and other applications, *J. Nanosci. Nanotechnol.* 11 (2008) 5993–6002.
- [40] B. Civalieri, P. Ugliengo, First principles calculations of the adsorption of NH₃ on a periodic model of the silica surface, *J. Phys. Chem. B* 40 (2000) 9491–9499.